Biosorption: Application Aspects – Process Simulation Tools

B. Volesky

Department of Chemical Engineering, McGill University, 3610 University Str.
MONTREAL, Canada H3A 2B2 boya@chemeng.lan.mcgill.ca

Recent research on metal biosorption has been elucidating its mechanisms and principles. For effective metal removal/recovery the process design has to be optimised for every type of application. That is most effectively done based on computer simulations utilizing mathematical models of the process. Some brief points of modelling methodology are summarized here.

1. Equilibrium Modeling

Biosorption has been studied with simplified sorption systems usually containing one heavy metal. This is quite appropriate simplification required for effective studies. Yu and Neretnieks[1] thoroughly reviewed model isotherms for single-component adsorption. Table 1 summarizes some of the most frequently applied simple sorption isotherm models.

Table 1: Frequently used single-component adsorption models

Isotherm	**Equation**	**Advant.**	**Disadvant.**	**Refer.**
Langmuir	$q = \frac{bq_m C_e}{1 + bC_e}$	Interpretable parameters	Not structured, Monolayer sorption	Langmuir (1918)[2]
Freundlich	$q = KC_e^{1/n}$	Simple expression	Not structured, no leveling off	Freundlich (1915)[3]
Combination (Langmuir-Freundlich)	$q = \frac{bq_m C_e^{1/n}}{1 + bC_e^{1/n}}$	Combination of above	Unnecessarily complicated	Sips (1948)[4]
Radke and Prausnitz	$\frac{1}{q} = \frac{1}{aC_e} + \frac{1}{bC_e{}^{\beta}}$	Simple expression	Empirical, uses 3 parameters	Radke & Prausnitz (1972)[5]
Reddlich – Peterson	$q = \frac{aC_e}{1 + bC_e{}^{n}}$	Approaches Freundlich at high concn.	No special advantages	Jossens *et al.*, (1978)[6]
Brunauer (BET)	$q = \frac{BCQ^{o}}{(C_s - C)[1 + (B - 1)C / C_s]}$	Multilayer adsorption; Inflection pt.	No "total capacity" equivalent	Brunauer (1938)[7]
Dubinin-Radushkevich	$\frac{W}{W_o} = \exp[-k(\frac{\varepsilon}{\beta})^2]$ (volume adsorbed)	Temperature independent: Polanyi pot'l. theory	Not limited behavior in the Henry's Law regime	Dubinin, (1947)[8]

There is no critical reason to use more complex models if 2-parameter models such as Langmuir and Freundlich isotherm can fit the data reasonably well. However, these models are just "mathematical functions", they hardly reflect the sorption mechanism. More structured types of models respecting sorbate speciation in solution, pH and even electrostatic attraction were recently suggested by Schiewer and Volesky[9,10,11] and Yang and Volesky.[12,13]

The most common sources of toxic metals, most conspicuous being acid mine drainage and electroplating effluents, contain a mixture of metals. For example, more than 30 different metals are dissolved in the Berkeley Pit in Montana, USA, threatening the nearby communities. For practical applications, multimetal biosorption models have to be judiciously used (Table 2).

Table 2: Frequently used multi-component adsorption models

Isotherm type	Equation	Advantages	Disadvantages	Reference
Langmuir (Multi-component)	$q_i = \frac{b_i q_{mi} C_i}{1+\sum_{i=1}^{n} b_i C_i}$	Constants have physical meaning. Isotherm levels off at max saturation	Not a "structured " Mpodel, does not reflect the mechanism well	Langmuir (1918)[2]
Combination Langmuir and Freundlich	$q_i = \frac{a_i C_i^{1/n_i}}{1+\sum_{i=1}^{N} b_i C_i^{1/n_i}}$	Flexible - better agreement with experimental data possible	Additional parameters used	Sips (1948)[4]
IAST: Ideal Adsorbed Solution Theory	$\frac{1}{q_t} = \sum \frac{Y_i}{q_i^o}$	Used by Najm *et al.* (1991)[14]; Crittenden *et al.* (1985)[15]	As reported by[6,16,17]	Radke and Prausnitz, 1972[5]
SCM: Surface Complexation Model (group)	$q \sim f(Ce)$ could follow e.g. Langmuir	Models more "structured" – intrinsicequilibrium constant could be used	Equilibrium constants have to be established for different types of binding	Yiacoumi & Tien (1995)[22]; Davis & Leckie (1978)[23]

So far there has been no attempt to describe ion-exchange adsorption equilibrium, such as the case may be in biosorption, by using the IAST. There are several authors[18,19,20] who took into account the non-ideality of ion-exchange resin by calculating the activity coefficients of each species in the solid phase using the Wilson model.[21]
The SCM uses a "surface" concept which may not quite apply to gel-based biosorption.

Surface Complexation Model (SCM)

The SCM is based on the concept of surface charge generated from the amphoteric surface sites, which are capable of reacting with sorbing cationic or anionic species to form surface complexes. According to the SCM, three separate steps are involved in metal ion adsorption: surface ionization, complexation between ionized sites and ionic species, and the establishment of an electrical double layer (EDL) next to the adsorbent surface.[22] Consequently, ions are attracted to charged surface in order to satisfy the electroneutrality constraint. Boltzmann factor is adopted to describe the distribution of ions:

$$N_i = N_{io} \exp\left(-\frac{z_i e \Psi_0}{kT} \right) \tag{1.1}$$

For a planar surface, the relationship between the surface charge density and electrical potential was derived from Poisson-Boltzmann equation which, at 25^{o}C (T=298K) when the dielectric constant of water is 78.5, can be reduced to:

$$\sigma = 0.1174 c^{1/2} \sinh(Z\Psi \times 19.46) \tag{1.2}$$

The most general model among SCMs is the two-pK triple-layer (TL) model[23] which assumes that electrical double layer consists of three parts divided by the surface plane (*o*-plane), the outer Helmholtz plane (*d*-plane) where diffusive double layer starts, and the inner Helmholtz plane (β-plane), the center where ions are located to form complexes with surface groups. All the possible equilibrium reactions between ions and surface functional groups (denoted by SOH) can be summarized by the following stoichiometry with the corresponding equilibrium constatnts:

$$\mathrm{SOH} + \mathrm{H}^+ \xleftrightarrow{K_{H1}} \mathrm{SOH}_2^+ \qquad \frac{[\mathrm{SOH}_2^+]}{[\mathrm{SOH}]\{\mathrm{H}^+\}} = K_{H1}\exp\left(-\frac{e\Psi_o}{kT}\right) \qquad 1(3\text{-}4)$$

$$\mathrm{SOH} \xleftrightarrow{K_{H2}} \mathrm{SO}^- + \mathrm{H}^+ \qquad \frac{[\mathrm{SO}^-]\{\mathrm{H}^+\}}{[\mathrm{SOH}]} = K_{H2}\exp\left(\frac{e\Psi_o}{kT}\right) \qquad (1.5\text{-}6)$$

$$\mathrm{SOH} + \mathrm{Cat}^+ \xleftrightarrow{K_{Cat}} \mathrm{SO}^-\mathrm{Cat}^+ + \mathrm{H}^+ \qquad \frac{[\mathrm{SO}^-\mathrm{Cat}^+]\{\mathrm{H}^+\}}{[\mathrm{SOH}]\{\mathrm{Cat}^+\}} = K_{Cat}\exp\left(\frac{e(\Psi_o - \Psi_\beta)}{kT}\right) \qquad (1.7\text{-}8)$$

$$\mathrm{SOH} + \mathrm{H}^+ + \mathrm{An}^- \xleftrightarrow{K_{An}} \mathrm{SOH}_2^+\mathrm{An}^- \qquad \frac{[\mathrm{SOH}_2^+\mathrm{An}^-]}{[\mathrm{SOH}]\{\mathrm{H}^+\}\{\mathrm{An}^-\}} = K_{\mathrm{An}}\exp\left(-\frac{e(\Psi_o - \Psi_\beta)}{kT}\right) \qquad (1.9\text{-}10)$$

The surface charges at *o*-plane and β-plane can be represented as:

$$\sigma_o = N\{[\mathrm{SOH}_2^+] + [\mathrm{SOH}_2^+\mathrm{An}^-] - [\mathrm{SO}^-] - [\mathrm{SO}^-\mathrm{Cat}^+]\} \qquad (1.11)$$

$$\sigma_\beta = N\{[\mathrm{SO}^-\mathrm{Cat}^+] - [\mathrm{SOH}_2^+\mathrm{An}^-]\} \qquad (1.12)$$

As the electroneutrality requires that $\sigma_o + \sigma_\beta + \sigma_d = 0$, the following can be expressed:

$$\sigma_d = N\{[\mathrm{SO}^-] - [\mathrm{SOH}_2^+]\} \qquad (1.13)$$

giving the total surface site density, N_s, as:

$$N_s = \frac{N}{F}\{[\mathrm{SOH}] + [\mathrm{SOH}_2^+] + [\mathrm{SOH}_2^+\mathrm{An}^-] + [\mathrm{SO}^-] - [\mathrm{SOH}^-\mathrm{Cat}^+]\} \qquad (1.14)$$

Parameters appearing in above equations, including the capacitance of electric double layer, equilibrium constants of surface reaction, surface area of sorbent and concentrations of functional groups can be obtained from a set of titration data. There are several computer algorithms designed for this purpose including FITEQL[24] and KINEQL.[22]

There are various ways of manipulating the TL model to simplified forms of SCMs. For example, it can be simplified to basic Stern (BS) model by merging β–plane and *d*–plane, which results in complexation taking place at the *d*–plane. At high ionic strength, the potential at *d*–plane (Ψ_d) converges to zero and thus, the BS model exhibits similar properties as the constant capacitance (CC) model. Those different models are summarized in Figure 1.[22]

The SCM possesses distinct advantages in that it can reflect equilibrium adsorption as a function of pH, ionic strength as well as the solute concentration. Furthermore, it also provides surface complexation constants, which are independent of varying solution conditions.[25]..In applying the SCM, there are several factors that need to be considered. Some metal ions form complex ions by hydrolysis reactions in aqueous solution. Sometimes, sorbing cations and anions also may form complexes in solution. Therefore, such solution complexation reactions also need to be taken into account in calculating surface complexation constants.[26] Also, at high concentrations of sorbing ions, surface precipitation may occur. Often it is hard to distinguish between adsorption and precipitation.[26,27] In high ionic strength solution, taking into account surface non-ideality is necessary, in which case treatment of activities rather than concentrations is desirable for each species involved in both solution reactions and surface reaction. Activity coefficients of each species involved in solution reactions can be calculated using Davies equation. Those involved in surface reactions are lumped into an exponential potential term appearing in the equation for surface complexation constants[25] (equations 1.4, 6,8,10 above).

Figure 1: Schematic description of Electrical Double Layer models

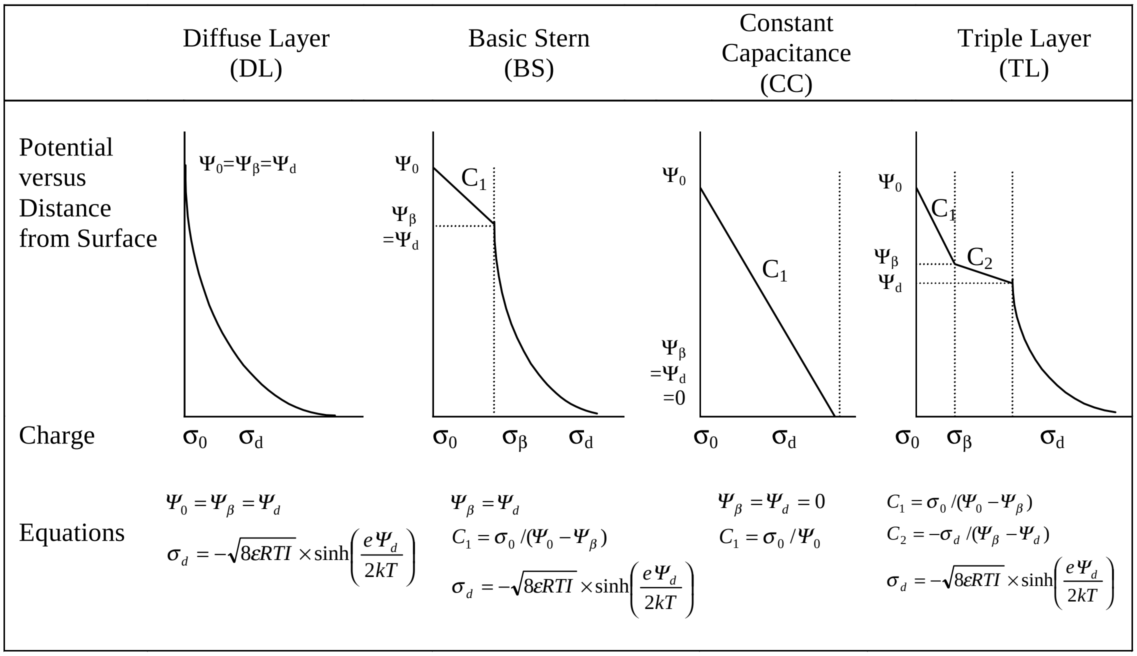

2. Biosorption dynamics in a continuous system

Most separation and purification processes that employ the sorption technology use continuous-flow columns. This operating mode ensures the highest possible concentration difference driving force. Starting at the inlet, the saturated solid sorbent zone gradually extends throughout the column., the sorbate eventually breaking through the column. The record of the breakthrough gives usually a typical s-shaped breakthrough curve whose shape and slope is the result of the equilibrium sorption isotherm relationship, the mass transfer to and throughout the sorbent in the column, and operation macroscopic fluid-flow parameters, such as axial mixing, affecting the deviation from the ideal plug flow.

The breakthrough time represents the duration of ongoing sorption until a pre-defined exit threshold sorbate concentration is reached. Any optimized column system is based on the accurate prediction of the breakthrough time under given specific operating conditions. When the sorbate concentration in the effluent stream reaches a pre-defined level, the column operation is terminated. At this point the regeneration process may begin before activation for the next cycle of operation.

2.1 Mass transfer model for continuous flow columns

The most important mass transfer resistance for sorption from aqueous solutions has been established to be the internal (intraparticle) diffusion.[28,29] The film resistance plays a less important role.[30,31] For column performance estimation, it is desirable to represent its behavior by an appropriate mathematical model which can be solved either analytically or numerically. The model can eventually also serve for optimising the column-based sorption process. A possible modelling methodology is outlined here is based on some assumptions:

1. The reaction time for sorption (i.e. binding to the functional group) is much shorter than that for diffusion of the ions through the biomass.

2. Chip-like *Sargassum* biomass particles are considered to be uni-dimensional thin plates. Therefore, the overall sorption rate is controlled by intraparticle diffusion in the direction normal to the surface of the particles.
3. The quantity of bound metal is in equilibrium with the metal concentration of the aqueous phase as formulated in the Langmuir sorption isotherm relationship.

During the biosorption process based on ion exchange the diffusion of metal ions into the biomass must be accompanied by the release of protons (or other ions) that diffuse into the bulk liquid. The diffusion coefficient for H^+ is several times higher than that for heavy metal ions present in infinitely diluted aqueous solutions[32,33]. Therefore, the assumption that the overall sorption rate is controlled solely by heavy metal diffusion is reasonable. Furthermore, Crist *et al.*[34] showed that the Langmuir isotherm model could be used for ion exchange rate calculations for algal biomass over a wide concentration range.

The mass conservation equation in the macroscopic fluid is represented by:

$$\varepsilon \frac{\partial C_b}{\partial \tau} + U_s \frac{\partial C_b}{\partial z} + \rho(1-\varepsilon)\frac{\partial \bar{q}}{\partial \tau} = 0 \tag{2.1}$$

Film mass transfer by:

$$\frac{\partial \bar{q}}{\partial \tau} = K_f a(C_b - C_r |_{r=R}) \tag{2.2}$$

Intraparticle diffusion by:

$$\varepsilon_p \frac{\partial C_r}{\partial \tilde{\tau}} + \rho \frac{\partial q}{\partial \tilde{\tau}} = D_e \frac{\partial C_r}{\partial r^2} \tag{2.3}$$

The sorption isotherm by:

$$q = f(C_r) \tag{2.4}$$

The initial and boundary conditions for equations (1) and (3) are as follows:

$$\tau \le 0, \quad C_b = 0 \qquad (0 \le z \le L) \tag{2.5}$$

$$z = 0, \quad C_b = C_{in} \qquad (\tau > 0) \tag{2.6}$$

$$\tilde{\tau} \le 0, \quad C_r = 0 \qquad (0 \le r \le R) \tag{2.7}$$

$$r = 0, \quad \frac{\partial c_r}{\partial r}\Big|_{r=0} = 0 \qquad (\tilde{\tau} > 0) \tag{2.8}$$

$$r = R, \quad D_e \frac{\partial c_r}{\partial r}\Big|_{r=R} = K_f (C_b - C_r |_{r=R}) \qquad (\tilde{\tau} > 0) \tag{2.9}$$

Since axial dispersion was neglected, the biosorbent at different axial positions within the column is exposed to the fluid at different times. Accordingly, the relationship holds:

$$\tilde{\tau} = \tau - \frac{\varepsilon z}{Us} \tag{2.10}$$

Defining a new corrected time $\theta = \tilde{\tau} = \tau - \frac{\varepsilon z}{Us}$ and substituting it into the above model equations, the following dimensionless relationships are obtained:

$$\frac{\partial u}{\partial x} + \beta \; Bo \; (u - v |_{y=1}) = 0 \tag{2.11}$$

$$\lambda(v) \frac{\partial v}{\partial t} = \frac{\partial^2 v}{\partial y^2} \tag{2.12}$$

$$t \le 0, \qquad u = 0 \qquad (0 \le x \le 1) \tag{2.13}$$

$$x = 0, \qquad u = 1 \qquad (t > 0) \tag{2.14}$$

x = 1 $$\frac{\partial u}{\partial x}\Big|_{x=1} = 0 \qquad (t>0) \tag{2.15}$$

t ≤ 0, $$v = 0 \qquad (0 \le y \le 1) \tag{2.16}$$

y = 0 $$\frac{\partial v}{\partial y}\Big|_{y=0} = 0 \qquad (t>0) \tag{2.17}$$

y = 1 $$\frac{\partial v}{\partial y}\Big|_{y=1} = Bo(u - v\,|_{y=1}) \qquad (t>0) \tag{2.18}$$

The definitions of new variables used in the above equations are as follows:

$$u = \frac{C_b}{C_{in}}, \qquad v = \frac{C_r}{C_{in}}, \qquad t = \frac{D_e}{R^2}\theta, \tag{2.19-21}$$

$$\gamma = \frac{D_e L}{U_s R^2}, \qquad \beta = (1-\varepsilon)\gamma, \qquad Bo = \frac{K_f R}{D_e}, \qquad \lambda(v) = \varepsilon_p + \rho\frac{\partial f}{\partial c}(c_{in}\, v) \tag{2.22-25}$$

It can be noted that a diffusion coefficient D_e is needed for calculations. It can be obtained, for instance, by regression fitting of the batch dynamics model as outlined by Yang.[35] This model, based on similar assumptions as above, the mass conservation and Langmuir sorption isotherm relationships, eventually becomes represented by the final matrix equation:

$$\left(\overline{\overline{M}} + \Delta t\overline{\overline{K}}\right)\vec{C} = \overline{\overline{M}}\vec{C}^{old} + \delta_{i,N}\,\omega\left(C_N - C_N^{old}\right) \tag{2.26}$$

Equation (4.2-26) is a linear equation with a tri-diagonal coefficient matrix and can be solved by a standard TDMA method.[36] A proprietary code in FORTRAN was prepared for running the algorithm.

2.2 Regression of model parameters

While the model parameters, K and q_m may be obtained from batch equilibrium experiments, all other parameters, except D_e , are known or may be calculated for a specific sorption contactor.[13,35] For the numerical solution of the model, the specific value of D_e corresponds to a specific simulated concentration profile of $\overline{C}(t)$ as a function of time and can thus be regressed from the comparison of the simulated profile curves and the experimental results by minimizing a given objective function. Simulations of biosorption rate were conducted for uranium and cadmium for chosen pH values. The resulting values for D_e are listed in Table 3.

Table 3: The regressed diffusion coefficients $\boldsymbol{D_e}$ (cm^2/sec)

Conditions:	pH 2.5	pH 3.0	pH 3.5	pH 4.0	Average
Uranium	4.0	6.0	6.0	6.0	5.5
Cadmium	6.0	5.0	6.0	6.0	5.75

The average diffusion coefficients for uranium and cadmium were $5.5\text{x}10^{-6}$ cm^2/sec and $5.75\text{x}10^{-6}$ cm^2/sec, respectively. These diffusion coefficient values are of the same order of magnitude as their respective molecular diffusivities, which are $7.21\text{x}10^{-6}$ cm^2/sec and $7.19\text{x}10^{-6}$ cm^2/sec respectively.[32,33]. Values for the effective diffusion coefficient may vary and can differ by several orders of magnitude even under similar experimental conditions. The calculated intraparticle diffusion coefficient is an effective diffusion coefficient, D_e, and it is usually smaller than the molecular diffusion coefficient D_m which is considered in the absence of the sorbent material matrix.

2.3 Numerical solution of continuous-flow column model equations

The dimensionless PDEs of the continuous-flow sorption process model can be solved numerically by the Orthogonal Collocation (OC) method.[37] This method, involving rather complicated discretizations and substitutions, cannot be fully elaborated on here. Instead, the following few statements abridge the procedure developed and described by Yang,[13] summarizing the results. Discretizing equations (2.11) (at axial collocation points, x_j) and (2.12) (at radial collocation points, y_{il}), . together with discretizing the radial boundary condition equations (2.16) and (2.17) prepared the latter set for the solution with respect to the boundary values V_{i1} and $V_{i,M+1}$ which were expressed[13] and eventually substituted into the discretized equation (2.12) yielding an expression for ($dv_{i,l}$ / dt). When U_i was eliminated from this equation and the axial boundary equations (2.14) and (2.15) discretized and solved for U_{N+1}, the resulting expressions can be substituted into the axial equation (2.19), expressing u_i with $v_{i,k'}$ as :

$$U_i = \sum_{j=1}^{N+1} D_{i,j}^{-1}\, e_j \tag{2-20}$$

Upon substituting this equation into a complex relationship for ($dv_{i,l} / dt$) the latter became a series of ODEs with respect to the interior radial concentration $V_{i,l}$.[12, 13] Thus with the initial condition $V_{i,l} = 0$, the key equation could be integrated over time by a standard integrating method such as the 4th order Runge-Kutta algorithm.[36] Once the $V_{i,l}$ s were obtained, the axial concentration U_i could be calculated from equation (2.20). A computer source code in FORTRAN was developed to implement the appropriate numerical algorithm.

2.4 Experiment modeling and model parameters determination

While the intraparticle diffusion coefficient D_e was determined by a batch dynamic study,[35] the film coefficient value K_f = 3.0x10^{-3} cm/s was regressed from experimental breakthrough curves.[35] Figure 2 illustrates experimental and model-calculated breakthrough curves for uranium ions sorbed by protonated *Sargassum* biomass at pH 2.5.

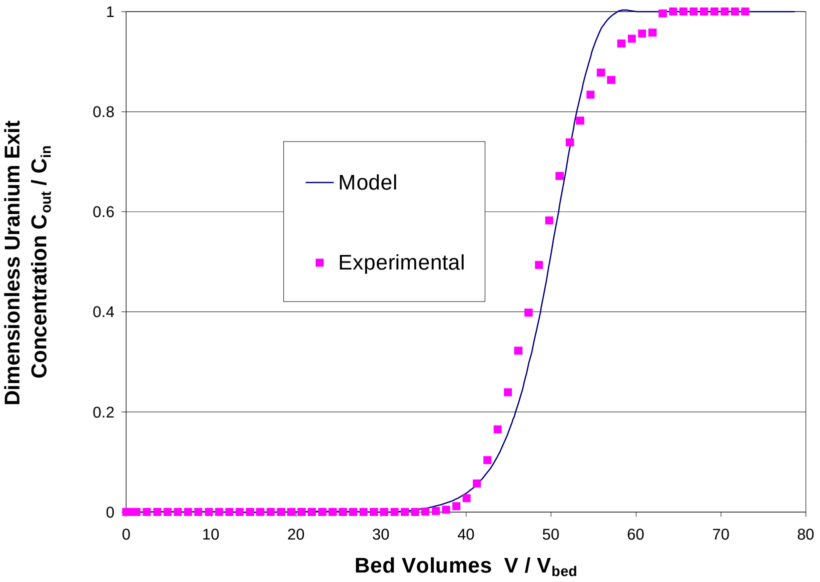

Figure 2: Comparison of experimental uranium breakthrough curve and the Mass Transfer Model calculated breakthrough curve for the protonated *Sargassum* biomass.

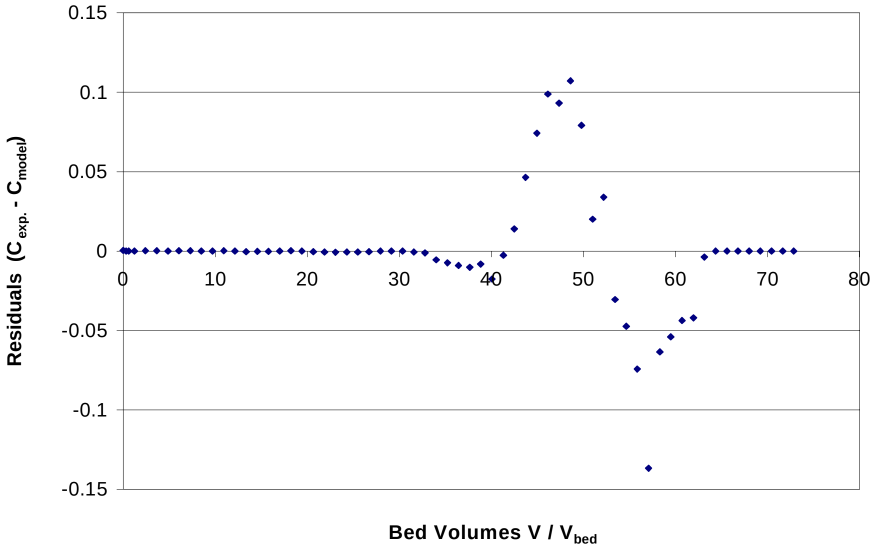

Figure 3: Residuals of the experimental and the Mass Transfer Model calculated uranium breakthrough curve.

The fitting curve was close to the experimental one within an average deviation of 5%. The trend in residuals is presented in Figure 3. The residuals for the "sorption" zone and for the "saturation" zone were minor. During the breakthrough process, the model did not statistically represent the experimental data very wel. However, the trend of the fitted curve agrees well with the experimental breakthrough data. The value of $K_f = 3.0 \times 10^{-3}$ cm/s, conveniently numerically regressed from the column experimental data, agrees well with the range obtained by Weber and Liu[38] (2.0 to 5.0×10^{-3} cm/sec) who used a "micro-column" technique. The model curve was not very sensitive to the external mass transfer diffusion coefficient, implying that only the intraparticle mass transfer was dominant.

2.5 Multi-metal biosorption column performance simulation

While the previous model simulation results can be applied to the biosorption process design and to optimize the operation of biosorption columns, it applies only to a single-metal system. To expand it to simulate the multimetal column operation is a very demanding task indeed. An example of the typical performance of a biosorption column with a multi-metal feed (Cu+Cd+Zn) is shown in Figure 4 together with a simulation attempt using a rare and proprietary software (IMPACT)[39] for a test-case with a biosorption column.

A laboratory-scale biosorption column with K-*Sargassum* biomass was fed with equimolar concentrations of Zn, Cd and Cu (1.0 meq/L). An exit concentration overshoot was conspicuous for Zn ($C/C_o > 2$ at $T > 1$). A slight increase in the effluent concentration of Cd followed the overshoot of Zn for a period that lasted until the breakthrough of Cu was complete.

This is because the relative affinities of Zn and Cd are much closer to each other (Zn/K = 1.965 and Cd/K = 3.706) than to Cu (Cu/K = 16.514). IMPACT program predicted breakthrough times (dimensionless time) for zinc and cadmium shifted ahead by approximately 20% when compared with the experimental data. While shifting it slightly ahead, IMPACT predicted 90% overshoot of Zn and 25% overshoot of Cd which agrees very well with the experimental results. The latest Cu breakthrough time could not be judged properly since the simulation stopped prematurely due to simulation calculation problems. The lack of information on the experimental software temporarily prevented continuation of this work.

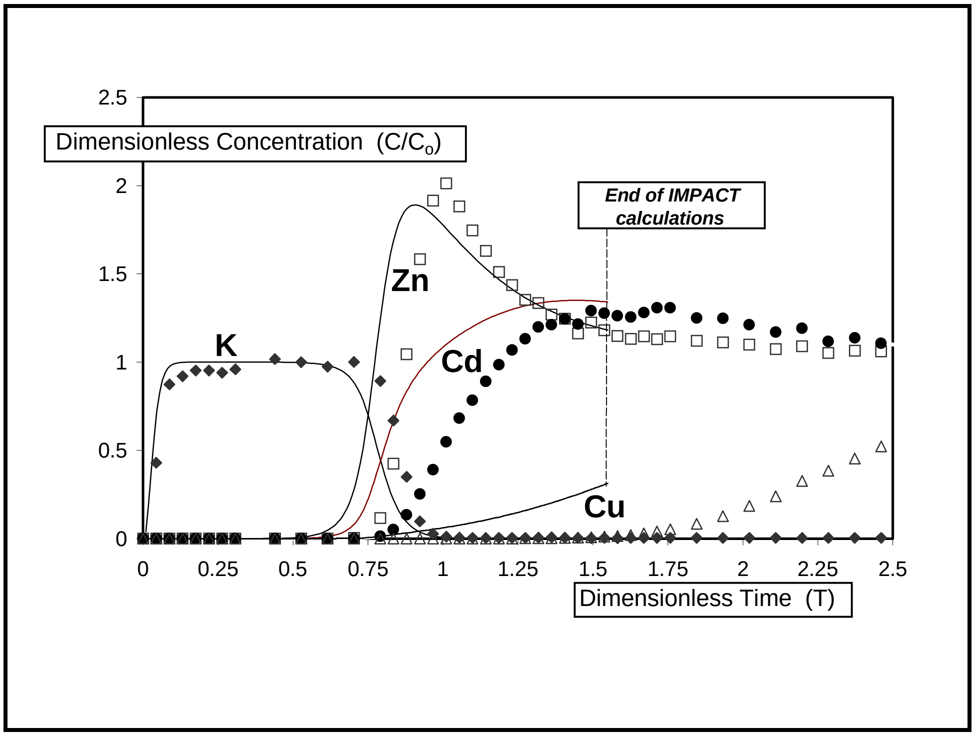

Figure 4: Results of the IMPACT biosorption process simulation (full lines).
Potassium pre-treated *Sargassum* - biosorption column performance.

However, it was encouraging to see that, to a certain degree, IMPACT could reasonably simulate the complex biosorption column performance within the limited scope of the work performed. While other mathematical models have been used for the same purpose, they are invariably only experimental and their computer versions are proprietary and difficult to use. For all practical purposes, the shape of the transition zone developed in the sorption column will determine the degree of the overall column utilization. This is the most important aspect when it comes to the economy of operation a column-based sorption process. There is no readily available sorption column performance simulation model which would incorporate all aspects of sorption, including equilibrium sorption relationships, mass transfer and fluid flow characteristics - and all this for multicomponent sorption systems. A ready-to-use and sophisticated enough process modeling software package would be extremely useful for biosorption performance estimation and process design. However, a suitable one is so far not available as yet.

3. Nomenclature

a	specific surface area of bisorbent particle (cm^{-1})
a, a_i	Langmuir isotherm parameter
b, b_i	Langmuir isotherm parameter
C_e	equilibrium solute concentration in fluid
C_b,	metal concentration in the bulk fluid stream
C_r	metal concentration in fluid of biosorbent pores
c	molar concentration
D_e	effective intraparticle diffusion coefficient (cm^2/sec)
e	electron charge
$f(C)$	the sorption isotherm relationship
K	intrinsic equilibrium constants (with subscripts)
K, n	Freundlich isotherm costants
k	Boltzmann constant
K_f	particle film mass transfer coefficient
N	F/Am where F is Faraday constant
q	uptake (mg/g)
q_i	uptake of i component (mg/g)
q^o_i	single-comp. adsorbed phase conc. in eq. with C^o_i
q_m	Langmuir maximum uptake (mg/g)
R	gas constant (or biosorbent particle radius (cm))
r	arbitrary position coordinate (cm)
T	absolute temperature
t	dimensionless time (-)
t, τ	time (sec)
U_s	fluid superficial velocity
$U_s = F/S$	(F - feed flowrate, S - column cross-area)

Y_i	solute concentration of *i* comp. in solid phase
Z	valence of ion
z	column axial coordinate (cm)
z_i	ionic charge of component *i*
α^i_j	separation factor between *i* and *j* species
β	Polanyi scaling factor in Polanyi models
ε	column bed porosity; Polanyi's adsorp. potential
ε_b	void factors of the fixed-bed column (-)
ε_p	intraparticle porosity (dimensionless)
ρ, ρ_p	biosorbent density (g/cm^3)
σ_d	charge density of *d*-plane
σ_o	charge density of *o*-plane
σ_β	charge density of β-plane
τ	time (sec)
Ψ	surface potential
Ψ_d	electric potential of *d*-plane
Ψ_β	electric potential of β-plane
Ψ_o	electric potential of *o*-plane

4. References

1. Yu, J-W and Neretnieks, I, 1990. *Ind. Eng. Chem. Res.* **29**, 220-231.
2. Langmuir, I, 1918. *J. Am. Chem. Soc.* **40**, 1361-1403.
3. Freundlich, H, 1907. *Z. Phys. Chem.* **57**, 385-470.
4. Sips, R, 1948. *J. Chem. Phys.* **16**, 490-495.
5. Radke, CJ and Prausnitz, JM, 1972. *J. AIChE* **18**, 761.
6. Jossens, L, Prausnitz, JM, Fritz, W, Schlunder, U & Myers, AL, 1978. *Chem. Eng. Sci.* **33**, 1097-1106.
7. Brunauer, S, Emmet, PH and Teller, E, 1938. *J. Am. Chem. Soc.* **60**, 309-319.
8. Dubinin, MM and Radushkevich, LV, 1947. *Chem. Zentr.* **1**, 875-.
9. Schiewer, S and Volesky, B, 1997. *Environ. Sci. Technol.* **31**, 2478-2485.
10. Schiewer, S, 1999. *J. Appl. Phycol.* **11**, 79-87.
11. Schiewer, S and Wong, MH, 1999. *Environ. Sci. Technol.* **33**, 3821-3828.
12. Yang, J and Volesky, B, 2000. *Environ. Sci. Technol.* **33**, 4049-4058.
13. Yang, J, 2000. PhD Dissertation, McGill University, Montreal, Canada.
14. Najm, IN, Snoeyink, VL and Richard, Y, 1991. *J. AWWA* **1991**, 57-63.
15. Crittenden, JC, Luft, P and Hand, DW, 1985. *Wat. Res.* **19**, 1537-.
16. Shivadji, S, 1995. *AIChE* **41**, 1135-1145.
17. Crittenden,JC, Luft,P, Hand,DW,Oravitz, JL,Loper, SW,Ari, M, 1985. *Envir.Sci.Technol.***19**, 1037-43.
18. Mehablia, MA, Shallcross, DC and Stevents, GW, 1992, in *Ion Exchange Advances, Proc. IEX'92*, Slater, MJ, ed. p. 151-158.
19. Smith, RP and Woodburn, ET, 1978. *AIChE J.* **24**, 577-587.
20. Shallcross, M, Herrmann, CC and McCoy, BJ, 1988. *Chem. Eng. Sci.* **43**, 279-288.
21. Wilson, GM, 1964. *Am. Chem. Soc. J.* **86**, 127-130.
22. Yiacoumi, S and Tien, C, 1995. *Kinetics of Metal Ion Adsorption from Aqueous Solutions: Models, Algorithms & Applications* (Kluwer Academic Publishers, Norwell, MA).
23. Davis, JA and Leckie, JO, 1978. *J. Colloid. Interface Sci.* **67**, 90-107.
24. Westall, JC & Morel,FMM,1997, in *Technical Note 19*, Ralph,M, ed. (Civ.Eng., MIT, Cambridge, MA).
25. Hayes, KF, Redden, G, Ela, W and Leckie, JO, 1990. *J. Coll. Interf. Sci.* **142**, 448-469.
26. Dzombak,DA & Morel,FMM, 1990.*Surface Complexation Modeling: Hydr. Ferric Oxide* (Wiley,NY).
27. Farley, KJ, Dzombak, DA and Morel, FMM, 1985. *J. Coll. Interf. Sci.* **106**, 226-242.
28. Rosen, JB, 1952. *J. Chem. Phys.* **20**, 387-394.
29. Apel, ML and Torma, AE, 1993. *Can. J. Chem. Eng.* **71**, 652-656.
30. Leusch, A and Volesky, B, 1995. *J. Biotechnol.* **43**, 1-10.
31. Tsezos, M, Noh, SH and Baird, MHI, 1988. *Biotechnol. Bioeng.* **32**, 545-553.
32. Dobos, D, 1994. *A Handbook for Electrochemists in Industry and Universities* (Elsevier), p. 88.
33. Horvath, AL, 1985. *Handbook of Aqueous Electrolyte Solutions* (Ellis Horwood, W.Sussex,UK),p.289.
34. Crist, RH, Martin, JR, Carr, D, Watson, JR, Clarke, HJ & Crist, DR, 1994. *Envir.Sci.Tech.* **28**, 1859-66.
35. Yang, J and Volesky, B, 1996. *J. Chem. Technol. Biotechnol.* **66**, 355-364.
36. Lapidus, L & Pinder, GE, 1982. *Numer. Solution of Partial Dif. Equations in Sci.&Engg.* (Wiley,NY).
37. Villadsen, J and Michelsen, M, 1978. *Solution of differential equation models by polynomial approximation* (Prentice-Hall, Englewood Cliffs, NJ), p. 111-143.
38. Weber, WJ and Liu, KT, 1980. *Chem. Eng. Commun.* **6**, 49-60.
39. Jausein, M, Andre, C, Margrita, R, Sardin, M and Schweich, D, 1989. *Geoderma* **44**, 95-113.